IEEE Access
Multidisciplinary | Rapid Review | Open Access Journal

Received 9 January 2024, accepted 4 February 2024, date of publication 7 February 2024, date of current version 16 February 2024.

Digital Object Identifier 10.1109/ACCESS.2024.3363645

RESEARCH ARTICLE

Compact Model of a Topological Transistor

MD. MAZHARUL ISLAM[1], (Graduate Student Member, IEEE), SHAMIUL ALAM[1], (Graduate Student Member, IEEE), MD. SHAFAYAT HOSSAIN[2], (Member, IEEE), AND AHMEDULLAH AZIZ[1], (Senior Member, IEEE)

[1]Department of Electrical Engineering and Computer Science, The University of Tennessee, Knoxville, TN 37996, USA
[2]Department of Physics, Princeton University, Princeton, NJ 08544, USA

Corresponding author: Ahmedullah Aziz (aziz@utk.edu)

This work was supported by the Air Force Research Laboratory under Agreement FA8750-21-1-1018.

ABSTRACT The precession of a ferromagnet leads to the injection of spin current and heat into an adjacent non-magnetic material. Besides, spin-orbit entanglement causes an additional charge current injection. Such a device has been recently proposed where a quantum-spin hall insulator (QSHI) in proximity to a ferromagnetic insulator (FI) and superconductor (SC) leads to the pumping of charge, spin, and heat. Here we build a circuit-compatible Verilog-A-based compact model for the QSHI-FI-SC device capable of generating two topologically robust modes enabling the device operation. Our model also captures the dependence on the ferromagnetic precision, drain voltage, and temperature with an excellent ($> 99\%$) accuracy.

INDEX TERMS Ferromagnetic, quantum spin hall insulator, superconductor, topological.

I. INTRODUCTION

The advent of transistors has unimaginably revolutionized the progression of human civilization in the last century. The consistent miniaturization of the transistor in the last few decades has made us capable of storing and processing vast amounts of data [1]. However, the quantity of data to be processed has also been increasing exponentially side by side [2]. While this dimensional reduction has taken place, researchers have already arrived at the theoretically predicted physical bottleneck [3]. In this context, topological materials stand in the spotlight for the exploration of future low-power and robust computational devices [4], [5]. The gapless surface state in topological insulators has made it a focal point of research [4], [6]. Although the technology is still in a nascent stage, there have been numerous remarkable efforts with significant research findings [7], [8]. Among them, there have been several propositions of the topological phenomenon-driven device structures [9], [10], [11], [12], [13]. Becerra et al. has recently proposed such a device where a quantum spin Hall insulator (QSHI) adjacent to a ferromagnetic insulator (FI) and a superconductor (SC) can harbor Majorana zero mode in the FI-SC junction [14]. This Majorana fermion (MF) enables topologically protected perfect Andreev reflection (AR) [15]. The precessing magnetization of the FI region enables interrelated and quantized spin, heat, and charge pumping. Here, the MF enables two unique topological operation regimes where the pumping of electrons can be turned on and tuned by external control parameters. In the low energy suppression regime, pumping is switched off due to the perfect AR of the electrons interacting with the MF hosted in the device. The perfection of AR, being topologically protected, renders this suppression unaffected by disorder or other imperfections in the device. Conversely, in the high-energy regime, the pumped charge becomes quantized due to the topological winding number associated with the scattering matrix, known as Thouless pumping. Consequently, operation in this regime is inherently robust against imperfections as well. Also, the injection of heat, spin, and charge is exponentially sensitive to the external control parameters (gate voltage, precession angle) similar to the conventional transistor behavior. Besides, the device offers sufficient scalability as QSHI can be patterned with FI and SC by various deposition methods [16], [17], [18], [19]. For these characteristic features, further circuit-level exploration is necessary. Hence, a physics-informed compact model can

The associate editor coordinating the review of this manuscript and approving it for publication was Lei Chen.

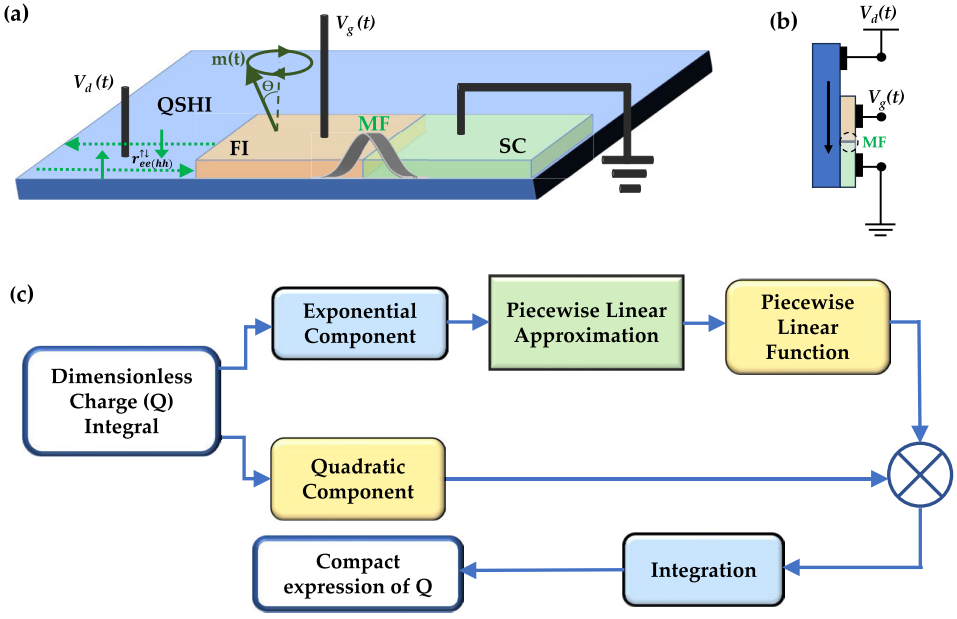

FIGURE 1. (a) The proposed device structure. A QSHI in proximity with the FI with a monodomain magnetization m(t) that precesses at an angle θ. In proximity to the FI region there is a SC region The monodomain magnetization *m(t)* precesses at an angle θ around the axis perpendicular to the QSHI. The QSHI region injects charge, spin, and heat currents to the drain. The injection can be controlled by the applied potential at the FI region (*Vg*), the precession angle (θ), precession frequency (ω) temperature (T) and drain voltage (V_d). Zero energy Majorana Fermion (MF) is harbored in the FI-SC interface that controls the pumped currents. (b) Circuit schematics for our simulation process. (c) Methodology flow for compact modeling.

serve as a handy tool to explore and generate valuable insights about the device that will leverage future research endeavors.

In this work, we develop a physics-informed compact model for the QSHI-FI-SC device. We simplify the rigorous mathematical expression of the injected spin, heat, and charge to a closed-form equation suitable for compact modeling. The piecewise linear approximation method is used to reduce the mathematical complexity. The deduced expression captures the dependency of the heat, spin, and charge injection on the external control parameters with great precision. Using the deduced closed form equation, we build a Verilog-A-based compact model. Our model can perfectly capture the proposed transistor behavior of the two topological regimes reported in [14]. Our model will enable the device and circuit-level exploration of the device. Besides, our modeling approach provides a pathway for future device modeling with a high level of mathematical complexity.

II. MODELING METHODOLOGY

To describe the system, the Bogoliubov-de Gennes Hamiltonian is considered as,

$$H_{BdG}(t) = [v_F p\sigma_z - \mu\,(x)]\tau_z + m(x,t).\sigma + \Delta(x)\tau_z \quad (1)$$

where $\sigma = (\sigma_x, \sigma_y, \sigma_z)$ and $\tau = (\tau_x, \tau_y, \tau_z)$ are the Pauli matrices acting on the spin and Nambu space. v_F is the Fermi velocity and *m(x,t)* is the time-dependent magnetization of the FI region. $\Delta\,(x)$ and μ(x) represent the superconducting order parameter and chemical potential, respectively. Throughout the whole SC region, $\Delta\,(x)$ is assumed to be constant as Δ_0. The *m(x,t)* is periodically driven in the FI region. This results in the pumping of the charge, spin, and heat in the left lead of the device (Fig. 1). The value of magnetization is parameterized as

$$m\,(x,t) = m_0\,(x)\,[\sin\theta\,(t).\cos\phi\,(t), \sin\theta\,(t).\sin\phi\,(t), \cos\theta\,(t)]$$

where $m_0(x) = m_0$ is the magnetization in the FI region. In the scattering matrix formalism, the only nonzero reflection co-efficient corresponds to the normal and Andreev reflections. Here, $r^{\uparrow\downarrow}_{he(eh)}\,(E,\,\theta,\phi)$ represent the reflection amplitude for the electron (hole) with spin $\downarrow$ injected from the QSHI to be reflected as a hole (electron). Again, $r^{\uparrow\downarrow}_{ee(hh)}\,(E,\,\theta,\phi)$ represent the reflection amplitude of the electron (hole) that has a spin $\downarrow$ and injected from the QSHI to be reflected as an electron (hole). These coefficients are related as $|r^{\uparrow\downarrow}_{ee(hh)}\,(E,\theta,\phi)\,|^2 + |r^{\uparrow\downarrow}_{he(eh)}\,(E,\theta,\phi)|^2 = 1$. The reflection coefficients can be expressed as, $r^{\uparrow\downarrow}_{ee(hh)}\,(E,\theta,\phi) = r_0(E,\theta)e^{i\phi}$ and $r^{\uparrow\downarrow}_{hh(ee)}\,(E,\theta,\phi) = -\,[r^{\uparrow\downarrow}_{ee(hh)}(-E,\theta,\phi)]^*$. At a sufficiently low energy, the magnitude of the coefficient representing the normal reflection is suppressed due to the perfect AR. In other words, at low energy, $|r^{\uparrow\downarrow}_{he(eh)}\,(E\,=\,0,\,\theta,\phi)|\,=\,1$, at low energy, the ϕ independent part can be approximated as

$$|r_0(E,\theta)|^2 \approx \frac{E^2/\Gamma^2}{1+E^2/\Gamma^2} \quad (2)$$

Here, Γ is the Majorana linewidth for which the normal and Andreev coefficients are equal. Γ is defined as-

$$\Gamma = 2\Delta_0\left(\frac{\xi_F\,(0,\theta)}{\xi_F\,(V_g,\theta)}\right)^2 \frac{\xi_S}{\xi_F\,(V_g,\theta)+\xi_S}\, e^{-\frac{2L}{\xi_F(V_g,\theta)}} \quad (3)$$

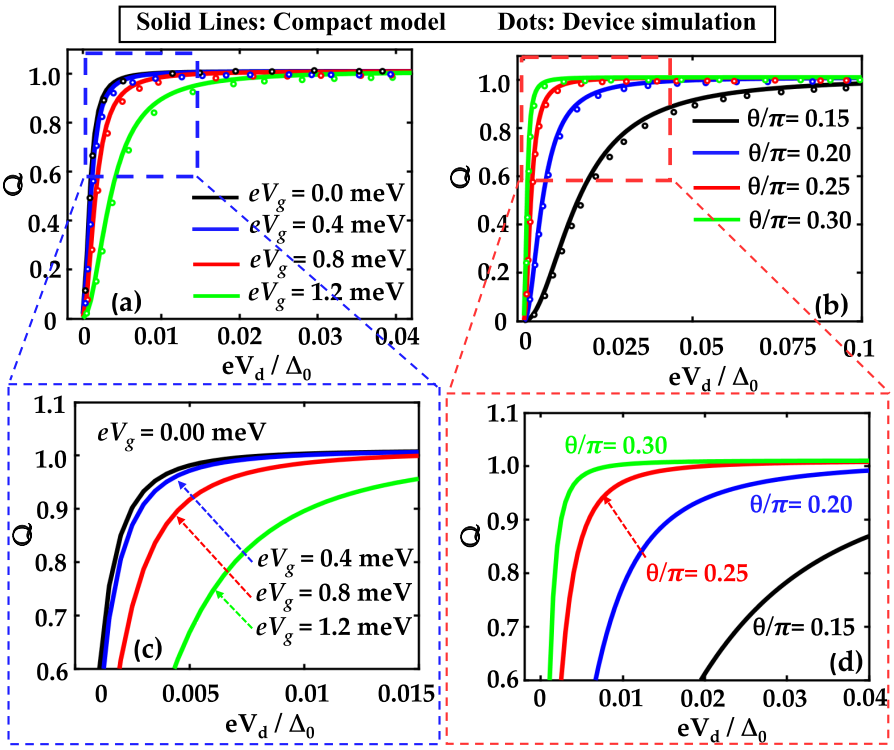

FIGURE 2. Drain voltage (V_d) dependence of the dimensionless charge (Q). The compact model characteristics are plotted alongside with the device simulation data (dotted data). Compact model (solid lines) accurately captures the datapoints from the device simulation (dotted brown). The dimensionless charge Q in the adiabatic limit as a function of V_d for various values of (a) V_g and (b)θ. (c)-(d). Compact model behavior zoomed into the transition region between two topological modes.

ξ_F and ξ_S are the coherence length of FI and SC region respectively. These can be expressed as, $\xi_F\left(V_g,\theta\right) = \frac{\hbar v_F}{\sqrt{(m_0^2\sin^2\theta-(eV_g)^2}}$ and $\xi_s\left(V_g,\theta\right) = \frac{\hbar v_F}{\Delta_0}$. The chemical potential of the FI region is controllable by the gate voltage (V_g) and is denoted as $\mu_{FI} = eV_g$. The length of the FI region is represented by L. The injection of charge, spin, and heat pumped in a single cycle can be described by a single parameter. This is referred as the dimensionless charge (Q) and is related to the charge, spin and heat as $Q_e = eQ$, $S_Z = -\frac{\hbar}{2}Q$, and $Q_E = -\frac{\hbar\omega}{2}Q$, respectively. The dimensionless charge Q can be expressed as:

$$Q = -\frac{1}{2\pi}\int dE\left(\frac{\partial f(E)}{\partial E}\right)\int_0^{2\pi} d\phi|r_{ee}^{\downarrow\uparrow}\left(E,\theta,\phi\right)|^2 \quad (4)$$

Thus, it depends on the Fermi energy (E_F) via the fermi function [$f(E)$] and the reflection coefficient ($r_{ee}^{\downarrow\uparrow}$). Q is sensitive to the temperature (T) and the applied drain voltage (V_d) via the Fermi function $f(E)$. It is also dependent on the rotation angle (θ) and the gate voltage (V_g) via $|r_{ee}^{\downarrow\uparrow}|^2$.

Now, taking the energy derivative of the Fermi energy and integrating $|r_{ee}^{\downarrow\uparrow}\left(E,\theta,\phi\right)|^2$, in the adiabatic limit, the dimensionless charge can be expressed as

$$Q = \int \frac{E^2 e^{\frac{E-(E_F+eV_d)}{kT}}}{kT\left(E^2+\Gamma^2\right)\left(e^{\frac{E-(E_F+eV_d)}{kT}}+1\right)^2}dE \quad (5)$$

The internal dynamics between the QSHI, FI, and SC are merged in equation (5) in an integral format. The integral expression is indefinite and is required to be expressed in a compact format to develop a circuit compatible Verilog-A model. To do so, we approximate the exponential component of the integrand. For simplicity, we are defining three different parameters as $\alpha = eV_d + E_F$, $\beta = kT$, $\gamma = \Gamma$. Now, the bell-shaped exponential component of equation (5) can be approximated as a piecewise linear function as below:

$$\frac{e^{\frac{E-\alpha}{\beta}}}{\left(e^{\frac{E-\alpha}{\beta}}+1\right)^2} = \begin{cases} 0; E < -3.8\beta+\alpha \\ 0.07\dfrac{E-\alpha}{\beta}+0.2660; -3.8\beta+\alpha < \&E < 0 \\ -0.07\dfrac{E-\alpha}{\beta}+0.2660; 0 < E < 3.8\beta+\alpha \\ 0; E > 3.8\beta+\alpha \end{cases} \quad (6)$$

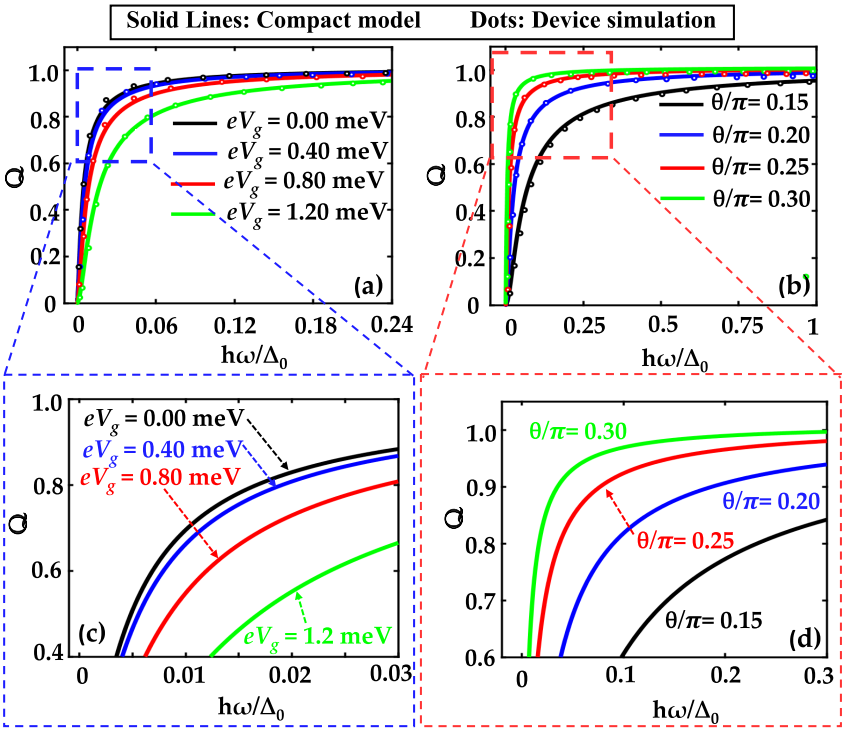

FIGURE 3. Precision frequency (ω) dependence of the dimensionless charge (Q). The compact model characteristics are plotted alongside with the device simulation data (dotted data). Compact model (solid lines) accurately captures the datapoints from the device simulation (dotted brown). The dimensionless charge Q in the adiabatic limit as a function of ω for various values of (a) V_g and (b) θ.(c)-(d). Compact model behavior zoomed into the transition region between two topological modes.

Now, Q over all possible energy range can be approximated as the following,

$$Q = \int_{-3.8\beta+\alpha}^{0} \frac{E^2}{\beta(E^2+\gamma^2)}\left(0.07\frac{E-\alpha}{\beta}+0.2660\right)dE + \int_{0}^{3.8\beta+\alpha} \frac{E^2}{\beta(E^2+\gamma^2)}\left(-0.07\frac{E-\alpha}{\beta}+0.2660\right)dE \tag{7}$$

Now, the result of the definite integral describes the closed form expression of the dimensionless charge as below,

$$\begin{aligned} Q=&\frac{1}{5000\beta^2}[175\gamma^2.\ln\left(\frac{25\gamma^2+361\beta^2-190\alpha\beta+25\alpha^2}{25\left(\gamma^2+\alpha^2\right)}\right) \\ &+(350\alpha-1330\beta).\gamma.[tan^{-1}(\frac{\alpha}{\gamma})+tan^{-1}(\frac{19\beta-5\alpha}{5\gamma})] \\ &+175\gamma^2.\ln\left(\frac{25\gamma^2+361\beta^2+190\alpha\beta+25\alpha^2}{25(\gamma^2+\alpha^2)}\right) \\ &+(350\alpha+1330\beta).\gamma.[tan^{-1}(\frac{\alpha}{\gamma})-tan^{-1}(\frac{19\beta+5\alpha}{5\gamma})] \\ &+2\times 2527\beta^2] \end{aligned} \tag{8}$$

TABLE 1. Device parameters for the QSHI-FI-SC structure.

Parameters	Values
Superconducting order parameters (Δ_0)	1 meV
Magnetization (m_0)	2 meV
Chemical potential (μ_0)	V_g - dependent (eV_g)
Fermi Velocity (v_F)	2.7×10^7 ms^{-1}
Length of the Ferromagnetic insulator region (L)	400 nm

III. SIMULATION RESULT

We calibrate our model with the geometric and material parameters corresponding to the QSHI-FI-SC structure reported in [14] (Table 1). Using equation (8), we build a circuit-compatible Verilog-A-based compact model. We validate our model with the device simulation result from [14]. Figure 2(a-d) shows the dependence of Q on V_d keeping all the other parameters at their nominal values. The device transforms from the topological suppression regime to the quantization regime as V_d goes from low to high voltage. It is evident that the model can capture the basic transistor behavior and matches with the device simulation results. Furthermore, the impact of V_g and θ on Q-V_d characteristics is also portrayed perfectly as evident from Figs.2 (a,b). For a certain V_d, Q decreases for higher V_g and increases with θ. Figs. 3(a-d) show the temperature dependence

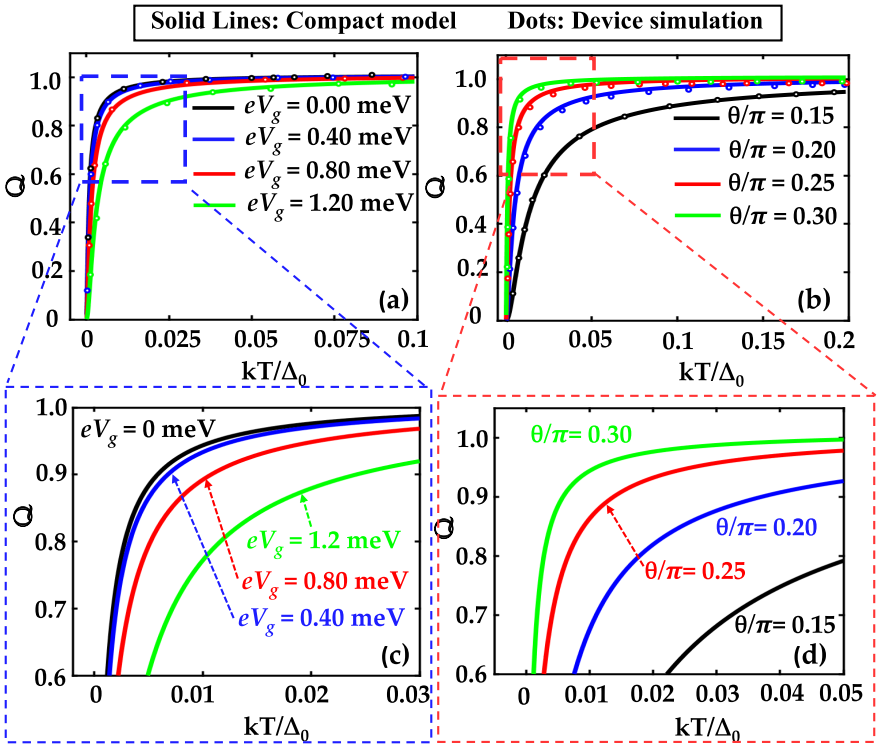

FIGURE 4. Temperature (T) dependence of the dimensionless charge (Q). The compact model characteristics are plotted alongside with the device simulation data (dotted data). Compact model (solid lines) accurately captures the datapoints from the device simulation (dotted brown). The dimensionless charge Q in the adiabatic limit as a function of T for various values of (a) V_g and (b) θ. (c)-(d). Compact model behavior zoomed into the transition region between two topological modes.

of Q. Here, Q increases with T and transfers from one (suppression) to another (quantization) topological regime as T increases. For a certain T, Q decreases with V_g and θ, and our model perfectly matches with the reported device simulation result (Figs. 3 (a) and (b), respectively). We also examine the variation of Q with respect to the ferromagnetic precision frequency (ω) as shown in Fig. 4(a-d). At lower ω, the device operates in the topological suppression regime and Q has a negligible value. On the contrary, at higher ω, Q has a high value owing to the high injection of spin current at the left lead. The excellent agreement between the theory and simulation results attests that our model can capture the ω variation as well. However, our model is limited in scope as it does not converge at 0 K, contrary to the theoretical device simulation. However, our model can describe the characteristics of Q for any other value of T and all possible values of ω and V_d. We set a miniscule nominal value of T (0.1 mK) for our simulation. As the device functions at a temperature below the critical temperature of the superconductor, the application of mV-range gate voltage does not pose any additional practical concerns. This is due to the negligible impact of thermal noise within the relevant temperature range (< 4.2 K). From Figs. 2-4, it can be said that our model matches with the theoretically demonstrated device simulation behaviors. The worst-case mismatch between the reported device simulation data and our model is $< 0.5\%$. s

IV. DISCUSSION AND CONCLUSION

In summary, we developed a compact model in Verilog-A for a QSHI-FI-SC structure via deriving a closed-form expression of the injected spin, heat, and charge by a piecewise linear approximation method. The model behavior is benchmarked with the device simulation to verify its functional behavior. Our Verilog-A model enables the future exploration of the circuit and system-level applications of the device. Our primary focus in this work is the compact modeling of the specific device discussed in our manuscript. Our objective is to create a circuit-compatible compact model that accurately captures the inherent physics of the device. Our circuit simulations serve to showcase the model's capability in precisely capturing the behavior related to injected charge, spin, and heat within the device. This precision enhances the model's applicability for investigating potential future applications of the considered device which remains as a future scope of research.

REFERENCES

[1] D. Burg and J. H. Ausubel, "Moore's law revisited through Intel chip density," *PLoS ONE*, vol. 16, no. 8, Aug. 2021, Art. no. e0256245, doi: 10.1371/journal.pone.0256245.

[2] T. Borgi, N. Zoghlami, M. Abed, and M. S. Naceur, "Big data for operational efficiency of transport and logistics: A review," in *Proc. 6th IEEE Int. Conf. Adv. Logistics Transp. (ICALT)*, Jul. 2017, pp. 113–120, doi: 10.1109/ICADLT.2017.8547029.

[3] S. Zhang, "Review of modern field effect transistor technologies for scaling," *J. Phys., Conf.*, vol. 1617, no. 1, 2020, Art. no. 012054, doi: 10.1088/1742-6596/1617/1/012054.

[4] L. Müchler, B. Yan, F. Casper, S. Chadov, and C. Felser, "Topological insulators," in *Thermoelectric Nanomaterials: Materials Design and Applications*, 2013, pp. 123–139.
[5] A. K. Pariari, "Atoms to topological electronic materials: A bedtime story for beginners," *Indian J. Phys.*, vol. 95, no. 12, pp. 2639–2660, Dec. 2021, doi: 10.1007/s12648-020-01925-x.
[6] Y. Ando, "Topological insulator materials," *J. Phys. Soc. Jpn.*, vol. 82, no. 10, Oct. 2013, Art. no. 102001, doi: 10.7566/jpsj.82.102001.
[7] S. Ma and S. M. Anlage, "Microwave applications of photonic topological insulators," *Appl. Phys. Lett.*, vol. 116, no. 25, Jun. 2020, Art. no. 250502, doi: 10.1063/5.0008046.
[8] M. He, H. Sun, and Q. L. He, "Topological insulator: Spintronics and quantum computations," *Frontiers Phys.*, vol. 14, no. 4, pp. 1–16, Aug. 2019, doi: 10.1007/s11467-019-0893-4.
[9] L. A. Wray, "Device physics: Topological transistor," *Nature Phys.*, vol. 8, no. 10, pp. 705–706, 2012.
[10] J. Michel, M. Mazharul Islam, M. F. Borunda, and E. Turgut, "Transportation of topological spin textures at material boundaries," *J. Magn. Magn. Mater.*, vol. 536, Oct. 2021, Art. no. 168088, doi: 10.1016/j.jmmm.2021.168088.
[11] S. Alam, M. M. Islam, M. S. Hossain, A. Jaiswal, and A. Aziz, "CryoCiM: Cryogenic compute-in-memory based on the quantum anomalous Hall effect," *Appl. Phys. Lett.*, vol. 120, no. 14, Apr. 2022, Art. no. 144102, doi: 10.1063/5.0092169.
[12] S. Alam, M. S. Hossain, and A. Aziz, "A non-volatile cryogenic random-access memory based on the quantum anomalous Hall effect," *Sci. Rep.*, vol. 11, no. 1, p. 7892, Apr. 2021, doi: 10.1038/s41598-021-87056-7.
[13] Z. Jiang, R. Li, S.-C. Zhang, and W. Liu, "Semiclassical time evolution of the holes from Luttinger Hamiltonian," *Phys. Rev. B, Condens. Matter*, vol. 72, no. 4, Jul. 2005, Art. no. 045201, doi: 10.1103/physrevb.72.045201.
[14] V. F. Becerra, M. Trif, and T. Hyart, "Topological charge, spin, and heat transistor," *Phys. Rev. B, Condens. Matter*, vol. 103, no. 20, May 2021, Art. no. 205410, doi: 10.1103/physrevb.103.205410.
[15] Y. Tanaka, T. Yokoyama, and N. Nagaosa, "Manipulation of the Majorana fermion, Andreev reflection, and Josephson current on topological insulators," *Phys. Rev. Lett.*, vol. 103, no. 10, Sep. 2009, Art. no. 107002, doi: 10.1103/physrevlett.103.107002.
[16] J. Huang, X. Duan, S. Jeon, Y. Kim, J. Zhou, J. Li, and S. Liu, "On-demand quantum spin Hall insulators controlled by two-dimensional ferroelectricity," *Mater. Horizons*, vol. 9, no. 5, pp. 1440–1447, May 2022, doi: 10.1039/d2mh00334a.
[17] A. Marrazzo and M. Gibertini, "Twist-resilient and robust ferroelectric quantum spin Hall insulators driven by van der Waals interactions," *Npj 2D Mater. Appl.*, vol. 6, no. 1, pp. 1–10, May 2022, doi: 10.1038/s41699-022-00305-9.
[18] L. Fu and C. L. Kane, "Josephson current and noise at a superconductor/quantum-spin-Hall-insulator/superconductor junction," *Phys. Rev. B, Condens. Matter*, vol. 79, no. 16, Apr. 2009, Art. no. 161408, doi: 10.1103/physrevb.79.161408.
[19] X.-L. Zhang, L.-F. Liu, and W.-M. Liu, "Quantum anomalous Hall effect and tunable topological states in 3D transition metals doped silicene," *Sci. Rep.*, vol. 3, no. 1, p. 2908, Oct. 2013, doi: 10.1038/srep02908.

MD. MAZHARUL ISLAM (Graduate Student Member, IEEE) received the B.S. degree in electrical and electronic engineering from the Bangladesh University of Engineering and Technology, in 2017. He is currently pursuing the Ph.D. degree in electrical engineering with The University of Tennessee Knoxville, TN, USA.

Since August 2020, he has been a Research Assistant with the Nanoelectronic Devices and Integrated Circuits (NorDIC) Laboratory. His research interests include beyond CMOS technologies and neuromorphic computing hardware in emerging devices.

Mr. Islam's awards and honors include the Tennessee's Top 100 Graduate Fellowship and the DAC Young Fellowship.

SHAMIUL ALAM (Graduate Student Member, IEEE) received the B.S. degree in electrical and electronic engineering from the Bangladesh University of Engineering and Technology, in 2017. He is currently pursuing the Ph.D. degree in electrical engineering with The University of Tennessee Knoxville, TN, USA.

Since January 2020, he has been a Research Assistant with the Nanoelectronic Devices and Integrated Circuits (NorDIC) Laboratory. His research interests include device modeling and circuit design for logic, memory, and in-memory computing applications at room temperature and cryogenic environments.

Mr. Alam's awards and honors include the Tennessee's Top 100 Graduate Fellowship, the DAC Young Fellowship, the Graduate Advancement Training and Education (GATE) Fellowship, and the Gonzalez Family Award for Outstanding Graduate Research Assistant.

MD. SHAFAYAT HOSSAIN (Member, IEEE) received the B.Sc. degree in electrical and electronic engineering from the Bangladesh University of Engineering and Technology, in 2013, and the Ph.D. degree in electrical engineering from Princeton University, Princeton, NJ, USA, in 2021.

He is currently a Postdoctoral Fellow with the Department of Physics, Princeton University. He works on experimental condensed matter physics where he uses experimental techniques to study many-body physics in two-dimensional electron systems.

AHMEDULLAH AZIZ (Senior Member, IEEE) received the B.S. degree in electrical and electronic engineering from the Bangladesh University of Engineering and Technology, Dhaka, Bangladesh, in 2013, the M.S. degree in electrical engineering from Pennsylvania State University, University Park, PA, USA, in 2016, and the Ph.D. degree in electrical and computer engineering from Purdue University, West Lafayette, IN, USA, in Fall 2019.

He is currently an Assistant Professor with the Department of Electrical Engineering and Computer Science, The University of Tennessee, Knoxville, TN, USA. Prior to beginning the graduate studies, he was a full-time Engineer with the Tizen Laboratory, Samsung Research and Development Institute, Dhaka. He was also a Co-Op Engineer (Intern) with the Technology Research Division, Global Foundries, Malta, NY, USA. His research interests include mixed-signal VLSI circuits, nonvolatile memory, and beyond CMOS device design.

Dr. Aziz received several awards and accolades for his research, including the Outstanding Dissertation Award from the European Design and Automation Association, in 2020, the Outstanding Graduate Student Research Award from the College of Engineering, Purdue University, in 2019, and the Icon Award from Samsung, in 2013. He was a co-recipient of two Best Publication Awards from SRC-DARPA STARnet Center, in 2015 and 2016, and the Best Project Award from CNSER, in 2013.